



Universiteit
Leiden
The Netherlands

Interaction of oxygen and carbon monoxide with Pt(111) at intermediate pressure and temperature : revisiting the fruit fly of surface science

Bashlakov, D.

Citation

Bashlakov, D. (2014, October 14). *Interaction of oxygen and carbon monoxide with Pt(111) at intermediate pressure and temperature : revisiting the fruit fly of surface science*. Retrieved from <https://hdl.handle.net/1887/29023>

Version: Corrected Publisher's Version

License: [Licence agreement concerning inclusion of doctoral thesis in the Institutional Repository of the University of Leiden](#)

Downloaded from: <https://hdl.handle.net/1887/29023>

Note: To cite this publication please use the final published version (if applicable).

Cover Page



Universiteit Leiden

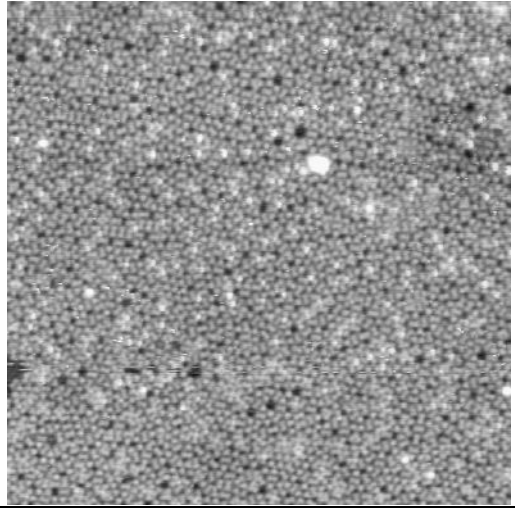


The handle <http://hdl.handle.net/1887/29023> holds various files of this Leiden University dissertation

Author: Bashlakov, Dmytro

Title: Interaction of oxygen and carbon monoxide with Pt(111) at intermediate pressure and temperature : revisiting the fruit fly of surface science

Issue Date: 2014-10-14



Chapter 4

Carbon monoxide oxidation on the Pt(111) surface at room temperature: STM and LEED studies

4.1 Introduction

The most important application of platinum as a catalyst is in the three-way catalytic convertor used in automobile exhaust systems [1]. Platinum is also considered a potential work horse in fuel cell vehicles, where chemical energy of a fuel is converted directly into electricity. A major obstacle for development of platinum-based low temperature fuel cells is poisoning (blocking) of active sites on the catalyst by impurities or strongly-bound reaction intermediates. Carbon monoxide is the most common example of such “poison”. The answer to the question “What chemistry occurs on the active (platinum) surface at the atomic scale?” under more realistic conditions may provide clues how the real catalyst can be modified to prevent poisoning.

Intensive fundamental studies of the interaction of platinum with carbon monoxide and oxygen started in the 1970’s with the development of surface science [2]. Numerous experimental techniques [3-14] were used to gather information regarding surface structures, adsorption positions, and energies of adsorbed species on platinum. These were supported by theoretical calculations [15, 16]. When summarizing the literature available for CO and O on the Pt(111) surface, we obtain the following picture.

Adsorption of carbon monoxide on the Pt(111) surface depends on the CO pressure and on exposure time [8, 13]. The least densely ordered structure, $(\sqrt{3}\times\sqrt{3})R30^\circ$, contains 1/3 ML of CO adsorbed on top of platinum atoms. Further adsorption leads to the more densely ordered $c(4\times 2)$ structure with 0.5 ML coverage where one half of CO molecules remains on top positions and the other half occupies bridge sites. Both commensurate structures were achieved at high vacuum conditions. An exposure of the surface to a higher CO pressure leads to the formation of an incommensurate layer (>0.5 ML) [6, 9].

At room temperature oxygen adsorbs dissociatively on clean Pt (111) via a molecular precursor [4, 17]. In this process two oxygen atoms have to be separated by two interatomic distances to complete the dissociation. After dissociation, the oxygen atoms occupy face cubic centered hollow sites [11, 18]. This leads to the formation of the $p(2\times 2)$ structure of atomic oxygen with 0.25 ML coverage [10, 12]. This structure is open for CO co-adsorption, thus a reaction to form CO_2 can proceed [7, 19, 20].

Steady state oxidation of carbon monoxide on Pt(111) has been studied at temperatures above 350 K [3, 21, 22]. It was shown that the

surface reveals two states characterized by a high and a low reaction rate, depending on the composition of the O₂:CO gas mixture and the surface temperature [22, 23]. Blocking (“poisoning”) of platinum by a CO adlayer was found to be responsible for the low reactivity regime. Lowering the concentration of carbon monoxide in the gas phase or increasing the sample temperature led to a distortion of the CO layer. This allowed molecular oxygen to find free sites needed for dissociation and the platinum surface switches to the high reaction state. This state is characterized by the presence of atomic oxygen on the surface [23, 24] and a sufficiently high CO→CO₂ conversion rate preventing surface poisoning. In contrast to steady state experiments, studies at room temperature and below were performed with a titration method, where the active Pt-O overlayer was replaced by a Pt-CO layer via the O_{ads}+CO_{ads}→CO₂ surface reaction [20, 25-27].

Despite abundant literature concerning ensemble-averaged studies of carbon monoxide oxidation on platinum, to date only one group had performed STM studies of this reaction at the atomic scale [26, 27], and only in a titration-type experiment. Furthermore, there is very little information available on the steady state oxidation reaction of CO on platinum at room temperature. In this chapter, we use STM and LEED techniques to visualize the processes on the Pt(111) surface in contact with various O₂:CO gas mixtures at room temperature. While LEED provides us with structural information over a large surface area, STM shows what happens locally at the atomic scale for the same conditions. Our study shows that the Pt(111) surface remains active toward CO oxidation at room temperature for CO concentrations ≤ 0.3%. STM reveals the formation of a complex surface structure under reactive conditions where islands of adsorbed atomic oxygen are separated by disordered areas. These topographic measurements are complemented by LEED patterns, showing the presence of a (2x2) oxygen structure on the Pt(111) surface at the same conditions.

4.2 Experimental section

Experiments were performed using a commercial “Omicron” UHV system consisting of preparation and analysis (reaction) chambers with a base pressure of 2×10^{-10} mbar. The Pt single crystal (6mm diameter and 1mm thick) was cut and polished within 0.1° precision of the (111) plane on

one side. A detailed description of the system as well as the initial sample cleaning and STM tip preparation procedures can be found in Chapter 2. Daily cleaning procedures included annealing in $3\text{-}4 \times 10^{-7}$ mbar of O_2 for 30 min at 900 K with subsequent heating to 1000-1100 K in vacuum for several minutes. Afterwards, the sample was transferred to the reaction chamber which was kept at UHV.

A gas mixture with the required $\text{O}_2\text{:CO}$ ratio was prepared in a separate mixing chamber equipped with a MKS121A Baratron capacitance manometer and leak valves. A schematic drawing of the dosing system is shown as an inset in Figure 4.1. This mixing chamber was separated from the reaction chamber via two valves with a small known volume in between. Dosing was performed by expansion of the prepared gas mixture from this small volume (3 mL, 1.2 Torr total pressure) into the reaction chamber (40 L). The latter was isolated from the pumps before gas mixture was admitted. It resulted in a total pressure of 1×10^{-4} mbar in the reaction chamber. The gases O_2 (Messer 5.0) and CO (Air Liquide 4.7) were used as supplied.

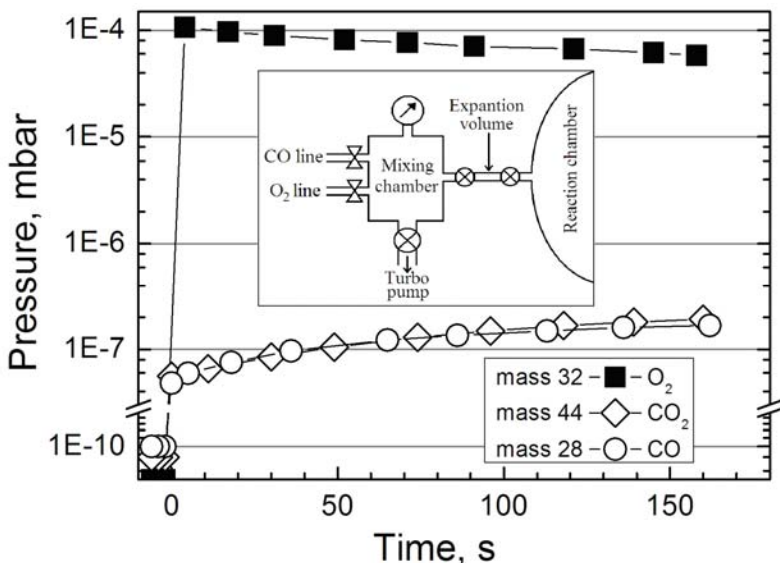


Figure 4.1 Evolution of the partial pressures in our deactivated reaction chamber after 1×10^{-4} mbar of oxygen was admitted at time=0 sec. The increase in the CO (CO_2) partial pressure is due to the production of these gases by the mass spectrometer's filament.

Our experiments were carried out in a “batch reactor” mode, where the entire UHV was backfilled with the gas mixture and sealed for the duration of the measurement. Vibration sensitivity of the STM precluded using the turbo pump for steady state gas flow conditions. Furthermore, we had to refrain from using the sublimation and ion pumps in the reaction chamber during the experiments due to their high chemical activity towards the constituents of the O₂:CO gas mixture. To keep the oxygen content stable, we had to deactivate titanium by keeping the analysis chamber under 1×10^{-4} - 1×10^{-3} mbar of O₂ for several hours after every bake-out. It sufficiently reduced the pumping speed of titanium and allowed us to use the analysis chamber as a closed reaction volume. Figure 4.1 demonstrates the changes in the oxygen pressure after backfilling the deactivated reaction chamber.

Ideally, the changes in the gas composition should be caused only by the catalytic reaction on the sample. However, we have noticed the presence of an additional source of CO and CO₂ in our reaction chamber when oxygen was admitted. From Figure 4.1 one can see that the amount of CO increases gradually and seems to saturate eventually. The filament of the quadrupole mass spectrometer (QMS) was responsible for this, since we observe the increase in the CO and CO₂ signals only when this filament is turned on in presence of O₂. Most probably, it is due to the oxidation of residual carbon present in the UHV chamber. Unlike the QMS filament, the LEED filament had no detectable influence on the contents of the gas mixture.

Mass spectrometry confirmed that the initial concentration of the admitted mixture of oxygen and carbon monoxide was the same as prepared in the mixing chamber. For example, dosing of the gas mixture with the smallest concentration of carbon monoxide used in our experiments (200:1 of O₂:CO) resulted in the initial $p_{\text{CO}} \approx 5 \times 10^{-7}$ mbar ($P_{\text{TOTAL}} = 1 \times 10^{-4}$ mbar).

Time needed to resolve the surface structure with LEED was limited only by the frame rate chosen to record the video. Measuring sample topography with STM required more time. Several tens of raster lines had to be collected to resolve the surface structures on Pt(111) terraces. With a scanning speed of 122-166 nm/s and a frame size of 30x30 nm² it took ~100 sec to obtain a two-dimensional image of the surface. From Figure 4.1 one can see that the composition of the gas mixture remains approximately constant within this time frame. Therefore, we could register changes in the surface structure even if they were caused by the variation in the composition of the gas mixture due to the influence of the chamber/filament.

Sample-to-tip drift correction was applied while scanning the clean platinum surface prior to its exposure to the gas mixture. Fast Fourier Transform (FFT) analysis revealed the 2.75 ± 0.2 Å interatomic distance for the clean Pt(111) surface confirming proper calibration of the piezo scanner. The distance between the nearest platinum atoms (2.77 Å) was also used as a reference for determining the periodicity of adsorbed species from the LEED images. From the analysis of the positions of platinum diffraction spots we found that our sample was retracted 11-12 mm from the geometrical focus of the LEED apparatus. We have taken this into account in our LEED structure calculations for the adsorbed overlayers. More details on the adlayer periodicity calculations were provided in Chapter 2.

4.3 Results and discussion

4.3.1 STM and LEED

The clean Pt(111) surface was exposed to O₂ or to a O₂:CO mixture of various compositions (10:1, 100:1 and 200:1) at $P_{\text{TOTAL}}=1\times 10^{-4}$ mbar. Changes in the surface structure were observed with STM and LEED during the exposure. We have to note for clarity that STM and LEED data were collected during separate dosing events. By synchronizing the measurements to the start of exposure to gases, local changes in the STM topography were correlated with the development of the diffraction patterns.

When the platinum surface was exposed to pure oxygen, rapid formation of an ordered structure in both STM and LEED measurements was observed as shown in Figure 4.2a. The ordering can be identified as the p(2x2) overlayer of atomic oxygen with 0.25 ML coverage [10, 12, 27]. Analysis of the STM and LEED images indicated 5.5 ± 0.35 Å and 5.3 ± 0.2 Å as the distances between nearest oxygen atoms, respectively. This is twice the distance between nearest platinum atoms (2.77 Å). This demonstrates that the presence of residual CO in our system does not influence oxygen adsorption.

The topography data in Figure 4.2b show the development of a different adlayer after the introduction of a 10:1 (O₂:CO) gas mixture. The diffraction data show exactly the same behavior where new patterns develop immediately after dosing. The orientation of these extra diffraction spots is rotated by 30° compared to the (1x1) diffraction features of the bare Pt(111) surface, indicating that the observed structure is formed by carbon

monoxide [6, 8]. The ordered structure on the topographic image in Figure 4.2b corresponds to a Moiré pattern formed by an incommensurate CO overlayer at this pressure [9]. The periodicity of the observed structure is $8.6 \pm 1 \text{ \AA}$ as derived from the FFT analysis of the current and subsequent STM images. The period of the Moiré structure defined from the LEED images is $8.0 \pm 0.6 \text{ \AA}$. Evacuating the chamber allowed resolving the CO structure with a periodicity of $3.7 \pm 0.1 \text{ \AA}$ [9, 28].

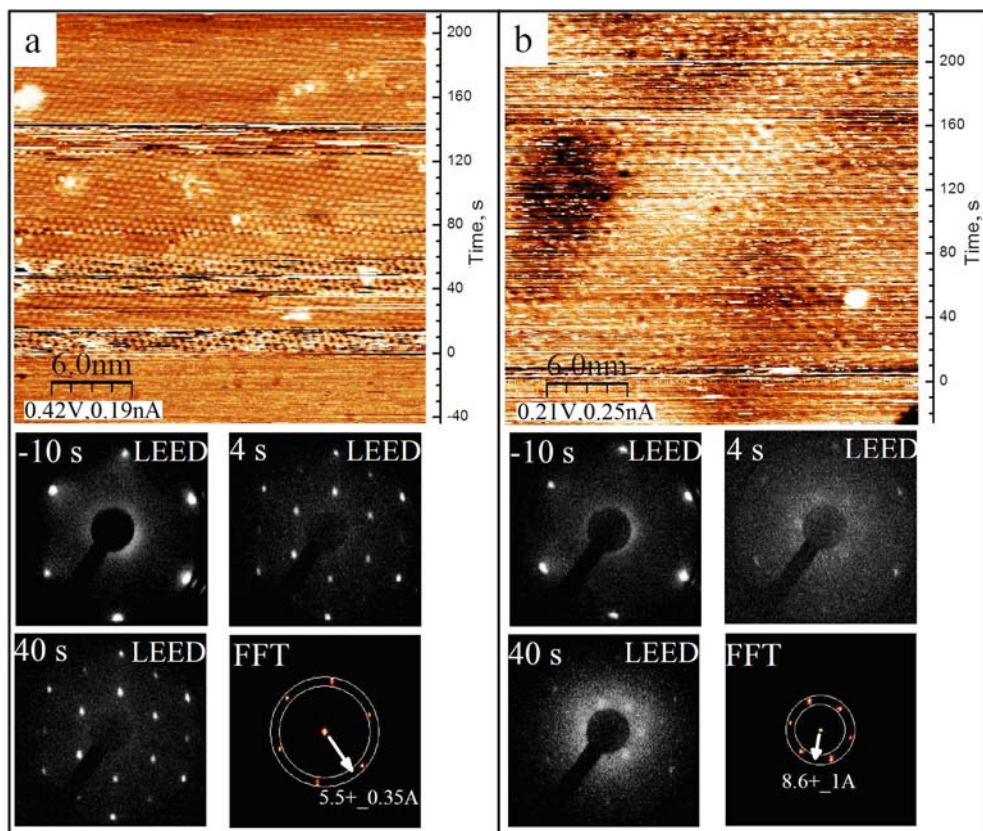


Figure 4.2. Changes in the surface structure of Pt(111) before and after exposure to clean oxygen (a), and a ($\text{O}_2:\text{CO}$) 10:1 mixture (b), recorded with STM and LEED. LEED snapshots, taken at 66 eV primary electron beam energy, are shown for the clean platinum surface ($t < 0$) and at certain times after gases were introduced into the reaction chamber. The bottom right images present FFT analyses of the STM data recorded after $t = 0$. Size of STM images is $26 \times 26 \text{ nm}^2$.

The Pt(111) surface adsorbs carbon monoxide faster than oxygen from the 10:1 mixture even though the number of CO molecules colliding with the surface is ten times smaller than for oxygen. This can be explained by the difference in the sticking probabilities ($S_{CO}=0.8-0.9$ [5, 20], $S_{O_2}=0.06$ [4, 14]) and the amount of available adsorption sites on Pt(111) for these gases. The clean platinum surface at room temperature can accommodate only 0.25 ML of oxygen but twice the amount of CO (0.5-0.68 ML depending on the CO pressure) [9, 12]. Even if some oxygen molecules are able to find a place to dissociate immediately after the clean surface has been exposed to the gas mixture, they will be removed by adsorbed CO through formation of CO_2 . Carbon monoxide will continue to dominate over oxygen for the adsorption position on the surface until no suitable sites for O_2 dissociation are left. Apparently, this happens so fast that both in the STM and LEED the formation of the CO overlayer from this mixture looks like simple carbon monoxide adsorption. Indeed we observe that exposing the Pt(111) surface to 1×10^{-5} mbar of pure CO (same pressure as P_{CO} in the 10:1 O_2 :CO gas mixture) leads to a rapid development of the Moiré pattern as is shown in Figure 4.3.

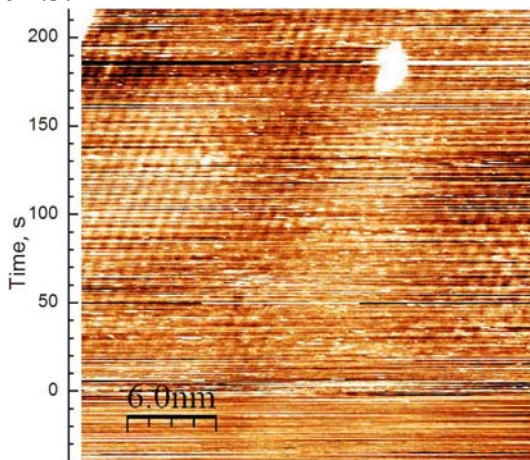


Figure 4.3 STM topography image of the Pt(111) surface $26 \times 26 \text{ nm}^2$ taken during its exposure at $t=0$ to 1×10^{-5} mbar of CO ($V=0.21$ V, $I=0.2$ nA).

The effect of CO domination over oxygen on the platinum surface remains even for the 100:1 (O_2 :CO) gas mixture as shown in Figure 4.4. The (2x2) oxygen structure forms immediately after the gases are introduced into the chamber and it takes a few seconds for CO to remove it. This means that oxygen has an initial advantage over carbon monoxide to adsorb on a clean platinum surface due to its higher concentration. The formed oxygen

adlayer is open for subsequent adsorption of CO [7, 19]. Further surface behavior is determined by the surface reaction and the competition of gas molecules for the available adsorption sites. A single reaction event clears up sites suitable only for the adsorption of carbon monoxide. Molecular oxygen, which adsorbs at room temperature only via dissociation, requires two adjacent surface sites which can only become available after the two nearest oxygen atoms recombine with CO molecules and leave the surface. The probability of such an event is determined by the amount and the type of molecules which arrive at the surface from the gas phase, i.e. the higher the CO content in the gas mixture, the higher the chance for CO to prevent O₂ dissociative adsorption. The concentration of carbon monoxide supplied from the 100:1 gas mixture to the platinum surface is apparently sufficient to poison the surface for oxygen dissociation. Thus, the diffraction patterns in Figure 4.4 show the development of the carbon monoxide overlayer with time.

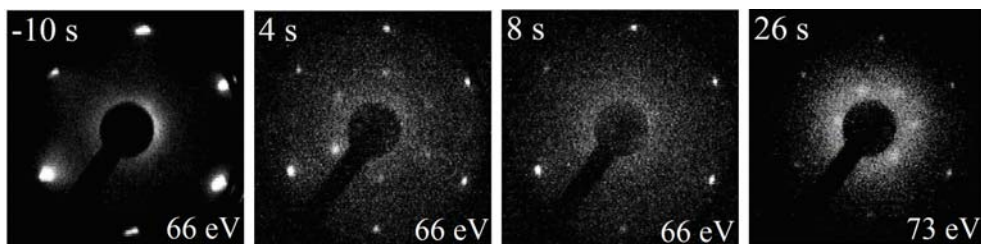


Figure 4.4. The snapshots of the LEED video recorded during the exposure of the Pt(111) surface to the 100:1 (O₂:CO) gas mixture.

We noticed two types of behavior while dosing a 200:1 (O₂:CO) mixture. The first type, shown in Figure 4.5a, has the same trends as for the 100:1 mixture but with a longer time needed for the formation of the CO overlayer. The topography data show first the formation of ordered oxygen islands which become disordered and then transform into the c(2x4) islands of CO. The second type, shown in Figure 4.5b, shows no switching to the carbon monoxide structure. The diffraction patterns of the p(2x2)-O adlayer become more pronounced with time. The STM image first shows the formation of patches of oxygen with disordered regions in between. The ordered oxygen layer is restored over the whole surface while the surface reaction reduces the CO concentration in the gas phase. We believe that the difference between these two cases is caused by the higher residual CO level in the reaction chamber for the first set of data, as will be shown below from the mass spectrometric data.

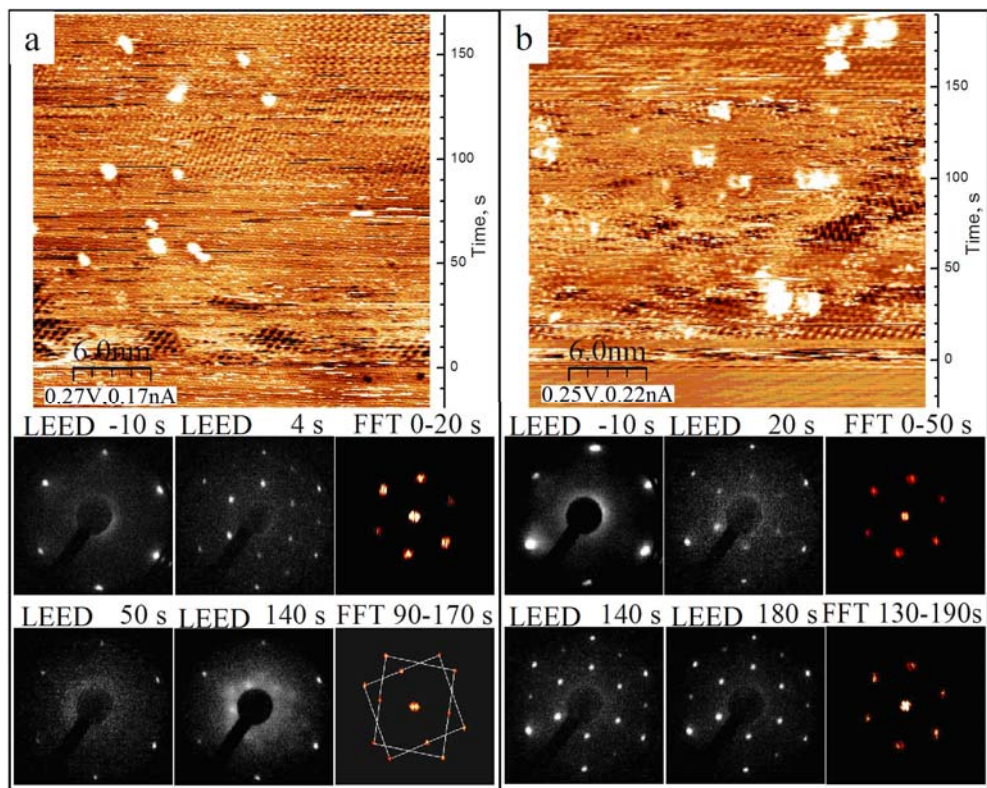


Figure 4.5 Changes in the surface structure of the Pt(111) exposed to the 200:1 (O_2 :CO) mixture showing the formation of the CO overlayer (a) and preservation of the active Pt-O layer (b) recorded with STM and LEED. The zero point on the time scale (right side of STM images) indicates the moment gases were admitted to the reaction chamber. FFT analysis from the top part of the topographic image (a) shows the presence of two $c(4 \times 2)$ -CO domains marked with squares. Size of STM images is $26 \times 26 \text{ nm}^2$. All LEED data were taken at 66 eV electron beam energy.

The results of topographic and diffraction measurements are summarized in Figure 4.6. The time periods during which the ordered CO layer or disordered surface were detected are marked with the black and gray bars, respectively. The white-hatched bars mark the time periods during which the (2×2) ordering of oxygen was observed. The response of the Pt(111) surface to the exposure to the O_2 :CO gas mixture can be divided in two steps. The first one describes the adsorption of the gases on the clean surface. This step is defined by the sticking probability of carbon monoxide ($S_{CO}=0.8$) and the dissociative adsorption probability ($S_{O_2}=0.06$) of oxygen

on Pt(111). Almost every molecule of carbon monoxide will adsorb upon collision with the platinum surface, while only 6% of the colliding oxygen molecules will adsorb and dissociate. That is why the p(2x2) oxygen structure develops only for gas mixtures with the CO concentration smaller than 10% ($O_2:CO=10:1$).

The second step includes the reaction between the atomic oxygen and carbon monoxide on the surface. No reaction is expected for the 10:1 mixture since the surface is blocked for the dissociative adsorption of molecular oxygen. However, the platinum surface covered with oxygen remains open for CO adsorption. The further process is defined by the competition of the molecules from the gas phase for the sites available after a single reaction event took place. The STM images from Figure 4.5 show that this competition leads to clustering on the surface where the p(2x2)-O islands are separated by disordered regions. The disordered regions presumably consist mostly of carbon monoxide [25, 27], which partially (or totally) blocks dissociation of molecular oxygen, as the structured CO adlayer is formed only after the unstructured regions spread over the whole platinum surface, which is shown in Figure 4.6 with grey bars.

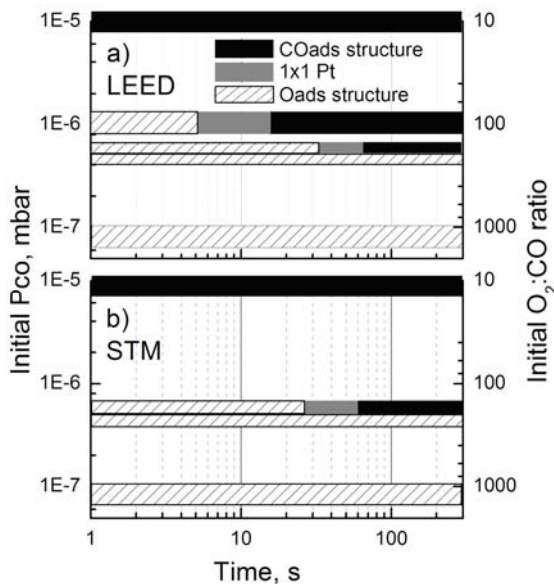


Figure 4.6 The time dependence for the adsorbate structures on the Pt(111) surface for different gas mixture compositions as observed with LEED (a) and STM (b) at a total gas pressure of 1×10^{-4} mbar. “1x1Pt” marks the region where no ordered structure of adsorbates was detected and only a diffraction pattern of Pt(111) was seen with LEED.

The energetically most stable adsorption site for carbon monoxide inside the ordered $p(2 \times 2)$ -O layer is on top of platinum atoms next to oxygen (non-O-bonded platinum atoms) [7]. The adsorption energy for co-adsorbed CO is almost the same as for the clean surface [15]. Also, the presence of carbon monoxide on top of platinum atoms does not change the chemisorption energy of oxygen atoms [15]. According to Alavi et al. [16] the situation changes if CO is displaced from the equilibrium position to the bridge site. It weakens the oxygen bond to one of the platinum atoms. Since the reaction barrier is defined by the strength of oxygen bonding to the surface, it thereby reduces the barrier for the reaction. Carbon monoxide has to leave the energetically favorable equilibrium position inside the $p(2 \times 2)$ -O overlayer to react. The situation is different on the periphery of oxygen islands. Carbon monoxide can already occupy the bridge sites in the oxygen free regions due to the higher concentration and the repulsive interaction between adsorbed CO molecules. It also can happen that the oxygen atoms are already displaced from these equilibrium three-hollow fcc sites due to thermal excitations. In both cases, the effective reaction barrier would be lower on the border of the $p(2 \times 2)$ -O island than in its interior. Therefore the reaction is expected to be more efficient on the oxygen island periphery.

The difference in reactivity of oxygen in the interior of the $p(2 \times 2)$ islands and at the borders was experimentally observed for the Pt(111) surface in oxygen titration experiments [25-27]. STM measurements carried out at 237-274 K showed that the reaction proceeds on the borders between ordered oxygen and carbon monoxide islands [26]. There it was also shown that some time (an induction period) needed for the formation of closely packed $c(4 \times 2)$. Nakai et al. [25] demonstrated two types of reaction kinetics for the same system. The first one was observed at 240 K when regions with high coverage of carbon monoxide coexist with the ordered oxygen islands, which was also confirmed by fast XPS [19]. In this case, the reaction takes place at the island's periphery in agreement with STM studies. The second type of reaction kinetics was observed at 350 K, where carbon monoxide accumulated on the surface only after oxygen had been removed. It was explained by thermally induced disordering of the $p(2 \times 2)$ -O islands [29]. However, the partial pressure of carbon monoxide in their experiments was rather low ($P_{CO} = 1 \times 10^{-8}$ mbar), and so it is quite possible that CO was removed by reaction with atomic oxygen faster than it was supplied from the gas phase, so that a two-phase interface could not be established. Wintterlin et al. [27] had to apply a CO pressure of 5×10^{-8} mbar at much

lower temperature (244 K) to form the $c(4 \times 2)$ -CO patches on the oxygen-free platinum surface. In the oxygen titration experiments of Campbell et al. [3] at 320 K with a molecular beam intensity corresponding to a CO pressure of 1×10^{-7} mbar, carbon monoxide was effectively removed by the surface reaction as fast as it was supplied to the surface.

Our STM results show that a densely packed carbon monoxide adlayer forms after the oxygen islands have disappeared (Figure 4.5a). This observation differs from previous STM studies at lower temperatures [26, 27] where both the $c(4 \times 2)$ -CO and $p(2 \times 2)$ -O structures were present on the surface simultaneously. It must be noted that the temperature used in our studies is closer to the desorption temperature of the $c(4 \times 2)$ -CO layer. The TPD peak starts around 300K [5, 6]. The potential energy surface is relatively flat for CO diffusion on Pt(111) [30, 31]. A one third monolayer of CO forms the ordered $(\sqrt{3} \times \sqrt{3})R30^\circ$ structure at 150 K where the CO molecules are on top of every third platinum as shown by Hopster and Ibach [8]. On the other hand, some amount (~ 0.1 ML) of the bridge sites was found to be occupied by carbon monoxide at 275 K even before the coverage reached $1/3$ ML [32]. Therefore, under our conditions carbon monoxide can freely migrate on Pt(111) and approach oxygen atoms for reaction before the formation of the densely packed CO adlayer. Another difference is that we have both reactants present in the gas phase. Competitive adsorption is taking place inside the disordered regions and at their borders. Disordered regions will turn into a CO or oxygen covered surface with time (Figure 4.5), depending on the (changes in the) $O_2:CO$ mixture composition.

4.3.2 Mass spectrometry

Using the reaction chamber as a closed vessel solved the problem of vibrations for the STM measurements. Yet if we look at the time evolution of the $O_2:CO$ ratio in the gas mixture (Figure 4.7), the influence of the reaction chamber on the partial pressure of the reactants becomes noticeable. Oxidation of residual carbon by the filament of the mass spectrometer appears as a decrease in the $O_2:CO$ mixture composition (increase in the CO partial pressure, cf. Figure 4.1) with time. Therefore the filament of the mass spectrometer was turned off shortly after the reaction mixture was introduced, and turned on again at the end (Δ, ∇ datasets with dashed lines). From Figure 4.7c one can see that this preserves the active

state of the surface and the amount of initially admitted CO reduces significantly until the filament is switched back on. Keeping the filament of the mass-spectrometer on for the 200:1 gas mixture resulted in surface passivation at 30 sec (\square dataset).

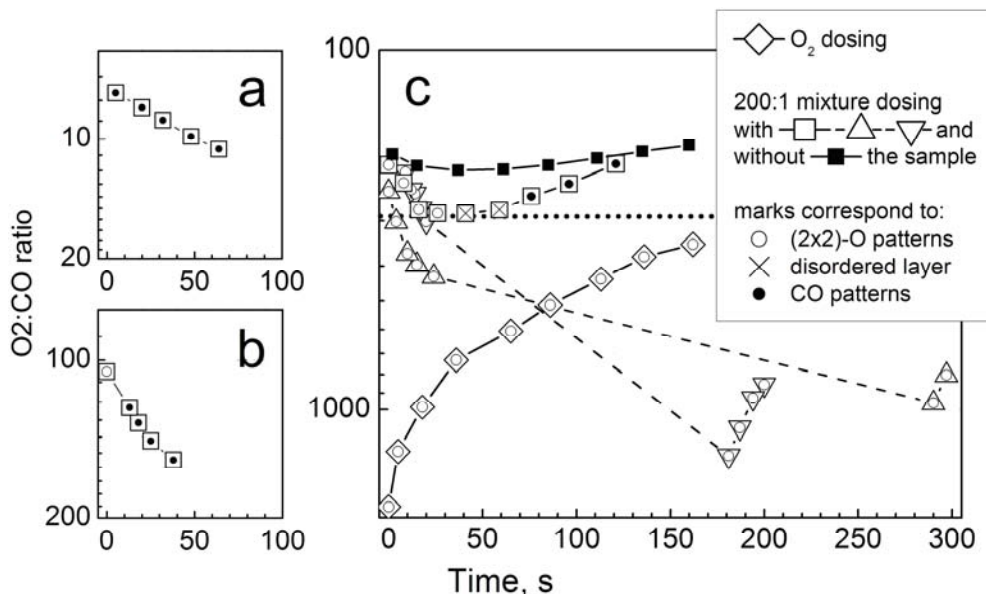


Figure 4.7 Changes in the $O_2:CO$ gas mixture composition with time during the LEED measurements for the 10:1 mixture (a), 100:1 mixture (b), 200:1 mixture (∇ , Δ , \square) and clean oxygen (\diamond) (c) admitted into the reaction chamber. $P_{total} = 1 \times 10^{-4}$ mbar. Data points marked with (\circ) correspond to the (2x2)-O LEED patterns. Diffraction patterns of the CO overlayer and unstructured surface adlayer (only (1x1) Pt(111) pattern visible) are marked with (\bullet) and (\times) symbols, respectively. The dataset with solid squares (\blacksquare) shows the evolution of the 200:1 gas mixture admitted into the reaction chamber without the sample. The dashed lines mark the time when the filament of the mass spectrometer was off.

Even so, we can clearly see that at certain composition of the gas mixture the active state of the platinum surface changes drastically. The dotted horizontal line marks the concentration of carbon monoxide which splits the graph in two regions. At higher concentrations CO tends to accumulate on the surface, in time forming a compact layer which blocks the dissociation of molecular oxygen and deactivates the catalyst. The active state of the surface covered by atomic oxygen is restored if the

concentration of CO is kept below 0.3 %. It is opportune to note that an extrapolation of data from Ehsasi et al. to our experimental temperature and pressure regime gives a very similar value for the concentration of CO at which the transition from high to low reactivity was observed [22].

4.3.3 Effect of CO poisoning on oxygen adsorption

Additional STM measurements were carried out to observe the effect of CO poisoning on oxygen adsorption on the Pt(111) surface. At the start of an experiment, the reaction chamber was filled with $2\text{-}3 \times 10^{-7}$ mbar of carbon monoxide to form the CO adlayer on the surface. The total pressure in the chamber was then increased to 1×10^{-4} mbar by dosing oxygen. Such a dosing sequence results in a more than 300 times higher partial pressure of O_2 than of CO. This O_2 :CO ratio is below the poisoning level for a clean platinum surface, according to the previous mass spectrometry data (Figure 4.7).

The adlayer structure was monitored continuously by scanning the same surface region before and after the O_2 admission and results are presented in Figure 4.8. As one can see no changes in the surface structure occur at the moment the surface was exposed to oxygen ($t=0$). Noticeable changes in the CO layer appear as a vanishing of the ordered structure after ≈ 550 seconds. The signature of oxygen presence appears even later (800-850 sec). The topography of this state is similar to what has been observed in Figure 4.5 in the transition period: small fractions of the oxygen-covered surface separated with disordered regions of carbon monoxide. This layer transforms rapidly into the complete layer of atomic oxygen.

Dissociation of oxygen is one of the elementary steps in oxidation reactions (see equations 1.1-1.3 for example). The presented data demonstrate that dissociation is inhibited by the presence of CO on the surface, which is in line with previous studies [23]. Although some reaction is still taking place, since the CO layer gets replaced with time by the oxygen layer. Based on our measurements, we cannot say which sites remain active for CO oxidation, when most of the platinum surface is covered with CO. But it is obvious that the reactivity of the overall surface is quite low. It takes time to release CO from the (111) terraces so oxygen can adsorb. At the same time, we observe that transitions from the low reactive state into the high reactive one (Figure 4.8) and vice versa (Figure 4.5) have the same atomic scale mechanism. In both cases, the adsorbates

tend to form an island-like structure on the Pt(111) surface in the transition phase.

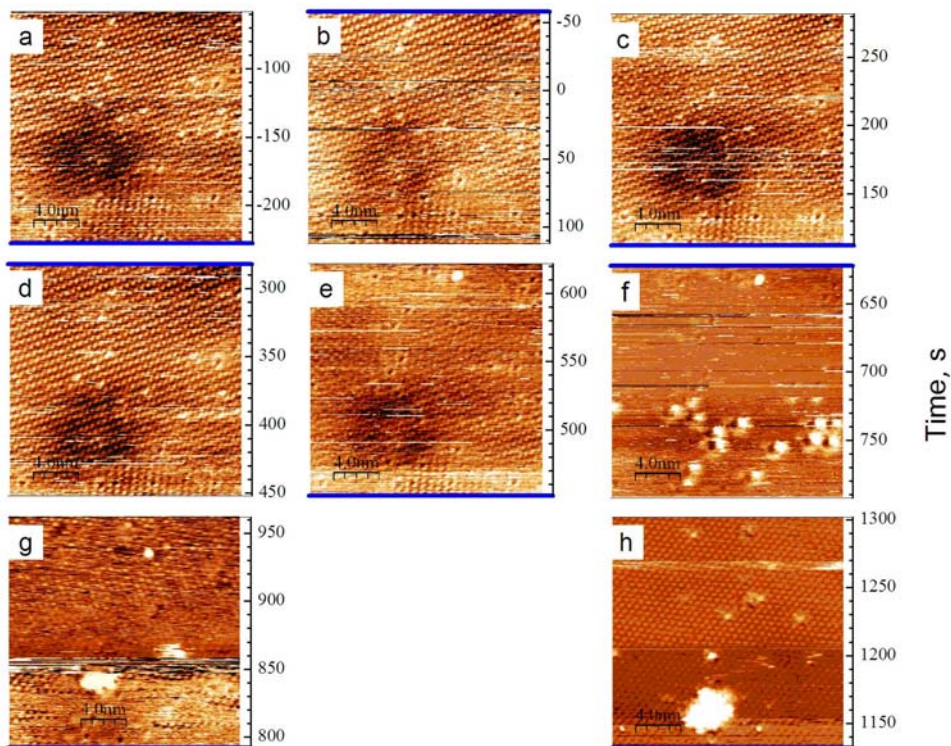


Figure 4.8 Consecutive STM images of the same Pt(111) surface area pre-covered with CO before (a-b) and after (b-h) oxygen has been admitted into the reaction chamber (time scale shown on the left side of each image). Images a-g were collected at $V=0.19V$ and $I=0.2nA$ and image h recorded at $V=0.35V$ and $I=0.14nA$. The moment 1×10^{-4} mbar of O_2 was introduced to correspond to $t=0$ sec (image b). Blue lines mark the first scan line of each topographic measurement. Voltage pulses have been applied to the tip to stabilize it after image (g) was recorded. Size of all images is $17 \times 17 \text{ nm}^2$.

4.4 Conclusions

At room temperature and 1×10^{-4} mbar gas pressure the catalytic oxidation of CO on Pt(111) was found extremely sensitive to the composition of gas mixture. STM and LEED measurements combined with mass spectrometry demonstrate that CO present at concentration above $\approx 0.3\%$ blocks the surface for the dissociative adsorption of oxygen, forming a dense ordered adlayer. At concentrations close to 0.3% carbon monoxide can be effectively converted into CO_2 without poisoning the surface, while Pt(111) demonstrates a complex surface structure with islands of atomic oxygen coexisting with disordered regions of carbon monoxide. The presence of such structure suggests that the oxidation reaction proceeds at the border of the oxygen islands, in agreement with previous titration experiments [25, 26]. Finally, if the concentration of CO in the (O_2 :CO) mixture is much less than 0.3%, the catalyst remains in its active state while its surface is covered with a compact $p(2 \times 2)$ layer of atomic oxygen. At room temperature adsorbed oxygen does not go subsurface on Pt(111), nor introduces surface oxidation or restructuring of this surface [33, 34], and adsorbed CO forms a compact monolayer unperturbed by thermally-induced desorption. No oscillations between the high and low activity states are observed, while the finite lifetime of the transition phase may be interesting to investigate at higher pressures [9].

References:

- [1] B. E. Nieuwenhuys, *Advances in Catalysis* 44 (1999) 259.
- [2] T. Engel and G. Ertl, *Advances in Catalysis* 28 (1979) 1.
- [3] C. T. Campbell, G. Ertl, H. Kuipers, and J. Segner, *The Journal of Chemical Physics* 73 (1980) 5862.
- [4] C. T. Campbell, G. Ertl, H. Kuipers, and J. Segner, *Surface Science* 107 (1981) 220.
- [5] C. T. Campbell, G. Ertl, H. Kuipers, and J. Segner, *Surface Science* 107 (1981) 207.
- [6] G. Ertl, M. Neumann, and K. M. Streit, *Surface Science* 64 (1977) 393.
- [7] J. L. Gland and E. B. Kollin, *Surface Science* 151 (1985) 260.
- [8] H. Hopster and H. Ibach, *Surface Science* 77 (1978) 109.
- [9] S. R. Longwitz, J. Schnadt, E. K. Vestergaard, R. T. Vang, I. Stensgaard, H. Brune, and F. Besenbacher, *The Journal of Physical Chemistry B* 108 (2004) 14497.
- [10] N. Materer, U. Starke, A. Barbieri, R. Doll, K. Heinz, M. A. Van Hove, and G. A. Somorjai, *Surface Science* 325 (1995) 207.
- [11] K. Mortensen, C. Klink, F. Jensen, F. Besenbacher, and I. Stensgaard, *Surface Science* 220 (1989) L701.
- [12] P. R. Norton, J. A. Davies, and T. E. Jackman, *Surface Science* 122 (1982) L593.
- [13] M. O. Pedersen, M.-L. Bocquet, P. Sautet, E. Legsgaard, I. Stensgaard, and F. Besenbacher, *Chemical Physics Letters* 299 (1999) 403.
- [14] Y. Y. Yeo, L. Vattuone, and D. A. King, *The Journal of Chemical Physics* 106 (1997) 392.
- [15] K. Bleakley and P. Hu, *Journal of the American Chemical Society* 121 (1999) 7644.
- [16] A. Alavi, P. Hu, T. Deutsch, P. L. Silvestrelli, and J. r. Hutter, *Physical Review Letters* 80 (1998) 3650.
- [17] B. C. Stipe, M. A. Rezaei, and W. Ho, *The Journal of Chemical Physics* 107 (1997) 6443.
- [18] J. Wintterlin, R. Schuster, and G. Ertl, *Physical Review Letters* 77 (1996) 123.
- [19] M. Kinne, T. Fuhrmann, J. F. Zhu, C. M. Whelan, R. Denecke, and H. P. Steinruck, *The Journal of Chemical Physics* 120 (2004) 7113.
- [20] F. Zaera, J. Liu, and M. Xu, *The Journal of Chemical Physics* 106 (1997) 4204.
- [21] H. Hopster, H. Ibach, and G. Comsa, *Journal of Catalysis* 46 (1977) 37.
- [22] M. Ehsasi, M. Matloch, O. Frank, J. H. Block, K. Christmann, F. S. Rys, and W. Hirschwald, *The Journal of Chemical Physics* 91 (1989) 4949.

- [23] M. Berdau, G. G. Yelenin, A. Karpowicz, M. Ehsasi, K. Christmann, and J. H. Block, *The Journal of Chemical Physics* 110 (1999) 11551.
- [24] J. H. Miners, S. Cerasari, V. Efstathiou, M. Kim, and D. P. Woodruff, *The Journal of Chemical Physics* 117 (2002) 885.
- [25] I. Nakai, H. Kondoh, K. Amemiya, M. Nagasaka, T. Shimada, R. Yokota, A. Nambu, and T. Ohta, *The Journal of Chemical Physics* 122 (2005) 134709.
- [26] S. Volkening and J. Wintterlin, *The Journal of Chemical Physics* 114 (2001) 6382.
- [27] J. Wintterlin, S. Volkening, T. V. W. Janssens, T. Zambelli, and G. Ertl, *Science* 278 (1997) 1931.
- [28] J. A. Jensen, K. B. Rider, M. Salmeron, and G. A. Somorjai, *Physical Review Letters* 80 (1998) 1228.
- [29] M. Nagasaka, H. Kondoh, I. Nakai, and T. Ohta, *The Journal of Chemical Physics* 122 (2005) 044715.
- [30] M. Lynch and P. Hu, *Surface Science* 458 (2000) 1.
- [31] E. Schweizer, B. N. J. Persson, M. Tushaus, D. Hoge, and A. M. Bradshaw, *Surface Science* 213 (1989) 49.
- [32] J. S. McEwen, S. H. Payne, H. J. Kreuzer, M. Kinne, R. Denecke, and H. P. Steinruck, *Surface Science* 545 (2003) 47.
- [33] D. Bashlakov, L. Juurlink, M. Koper, and A. Yanson, *Catalysis Letters* 142 (2012) 1.
- [34] C. Ellinger, A. Stierle, I. K. Robinson, A. Nefedov, and H. Dosch, *Journal of Physics-Condensed Matter* 20 (2008)

